

## HIGH-CAPACITY TRANSPORT IN CITIES AND THE IMPACT ON THE ROADS



**S. RAHMAN**  
Senior researcher, VTI,  
the Swedish National  
Road and Transport  
Research Institute,  
Linköping, Sweden.  
Obtained his Ph.D from  
KTH Royal Institute of  
Technology, Sweden.



**S. KHARRAZI**  
Senior researcher, VTI,  
the Swedish National  
Road and Transport  
Research Institute,  
Linköping, Sweden.  
Obtained her Ph.D from  
Chalmers University of  
Technology, Sweden.



**S. ERLINGSSON**  
Professor, VTI, the  
Swedish National Road  
and Transport Research  
Institute, Linköping,  
Sweden.  
Obtained his Ph.D from  
KTH Royal Institute of  
Technology, Sweden.

### Abstract

This paper presents the evaluation of the relative pavement damage caused by a high-capacity transport (HCT) 5-axle truck with respect to three other reference trucks consisting of 4, 3 and 2 axles. The analysis was conducted by simulating the responses of three pavement structures using the pavement analysis tool ERAPave. Two damage criteria of the pavement structures were considered: fatigue cracking of the asphalt concrete (AC) layer and permanent deformation of the subgrade. The relative damage caused by the different vehicles were estimated by calculating a damage factor ( $D_r$ ) following the Asphalt Institute Method. Three loading scenarios of the trucks were analyzed: (a) one way trip with fully loaded trucks, (b) round trip where the return trip consisted of the empty vehicles with lifted axles and (c) round trip where the return trip consisted of the empty vehicles without lifting any axles. The damage factors were calculated per unit carried load with respect to the 2-axle truck. Results indicate that the relative impacts of the vehicles depend on the structure type and season. Based on calculations of the yearly damage factors, the HCT truck appeared to be less damaging than the 3-axle and the 2-axle trucks, but slightly more damaging than the 4-axle truck. Weighing in other benefits, the HCT truck may be a better option than all the reference vehicles.

**Keywords:** High-capacity transport, pavement damage, damage factor, fatigue cracking, subgrade rutting, axle load, payload, fuel consumption, emissions

## **1. Introduction**

The construction industry is responsible for about 40% of energy use and one third of the greenhouse emissions world-wide (Fredriksson et al., 2021). Sezer and Fredriksson (2021) estimated that about 10% of these emissions stem from the transport of mass in connection with constructions. Thus, increasing efficiency of construction transport by improved logistic solutions and more efficient vehicles is of vital importance.

Roughly 20% of the Swedish goods transport relate to construction and infrastructure projects, but in urban areas as much as 50% weight-restricted transport is connected to constructions (Cederstav et al., 2022). To address the need for more efficient construction transport in cities, a pilot project on using high-capacity transport (HCT) vehicles for excavated material in urban areas in Sweden started in spring 2021. The project is called HCT City and includes partners from industry, city planners, universities, and research institutes. The term HCT is used to refer to heavy vehicles which are heavier/longer than the existing vehicles on the road network, allowed by regulations.

The roads in Sweden are divided into four classes of bearing capacities (called BK classes in Sweden). The allowed weight of the vehicle on each road depends on the distance between the first and last axle of the vehicle and the bearing capacity class of the road. The maximum allowed gross weight is 64 ton for BK1, 51.4 ton for BK2, 37 ton for BK3, and 74 ton for the recently added class of BK4 (Swedish Transport Agency, 2018). The maximum allowed length for heavy vehicles is 25.25 m, but there are plans to allow longer vehicles up to 34.5 m on part of the road network. Within several cities in Sweden, local restrictions on the weight and length of heavy vehicles exist. A common restriction in inner cities is a maximum length of 12 m and bearing capacity of BK2 which implies in practice a maximum weight around 25 ton for a truck where the distance between its first and last axles is around 7 m (Treiber and Bark, 2018).

In the HCT city project, two construction sites are used as pilots, one of which is in Stockholm, where excavations are going on for a new residential area. Specially designed 5-axle trucks with gross weight of 38-42 tons and a length under 12 m will be used for transport in connection to this site. That means the payload capacity will be doubled in comparison to common 3-axle trucks complying with the BK2 bearing capacity. According to an earlier study, such a solution has the potential of reducing fuel consumption by 50% (Treiber and Bark, 2016). However, there are concerns about the impact of the HCT 5-axle trucks on road wear. Therefore, as part of the project, a simulation study on the effects of HCT 5-axle truck on road wear, in comparison with three reference trucks was performed. Three pavement structures representative of Stockholm urban area were used in the simulations. Also, five seasons based on pavement temperature measurements were considered. The outcomes of this study are presented and discussed in this article.

## **2. Methodology**

The objective of this work is to compare the risk of pavement damage induced by the HCT truck with three reference trucks, shown in Figure 1. The study was carried out by simulations using a pavement analysis tool called ERAPave (Elastic Response Analysis of Pavements), developed by the Swedish National Road and Transport Research Institute (Erlingsson and Ahmed, 2013; Ahmed and Erlingsson, 2015). Three hypothetical pavement structures,

representative of Stockholm urban area, were analyzed. These three structures comprised of asphalt concrete (AC) layers with different thicknesses (relatively thin, intermediate, and relatively thick) to cover the possible variations that may be encountered along the route of the trucks. The analyses were carried out for five seasons. Layer and material properties of the pavement structures required for the analyses were based on typical values determined from laboratory tests and historic data.

The analyses were conducted considering the viscoelastic behavior of the AC materials. The unbound layers were assumed to follow a linear elastic behavior. The vehicles were modelled using the axle load and spacing, tire pressure, tire configuration and speed. For each passage of the vehicles, the stresses and strains developed in the different layers were calculated and the relative damages caused by the different vehicles were evaluated and compared. It was assumed that the stresses are distributed over a circular tire-pavement contact area, the size of which was determined based on the axle load and tire pressure. In other words, the effect of tire width on the contact area was not modelled.

Three scenarios were analyzed: (a) one way trip with fully loaded trucks, (b) round trip where the return trip consisted of empty vehicles with lifted axles and (c) round trip where the return trip consisted of empty vehicles with all axles on the ground.

## 2.1 Description of the trucks

The HCT truck has 5 axles, is 10.75 m long and can carry 23.5 tons of load. The reference trucks have 2-4 axles, are 7.08-8.66 m long and can carry 7-18 tons, see Figure 1. The HCT truck has an extra steerable axle at the front, about 2 m behind the front axle. Other relevant parameters of the trucks and their tires are listed in Table 1.

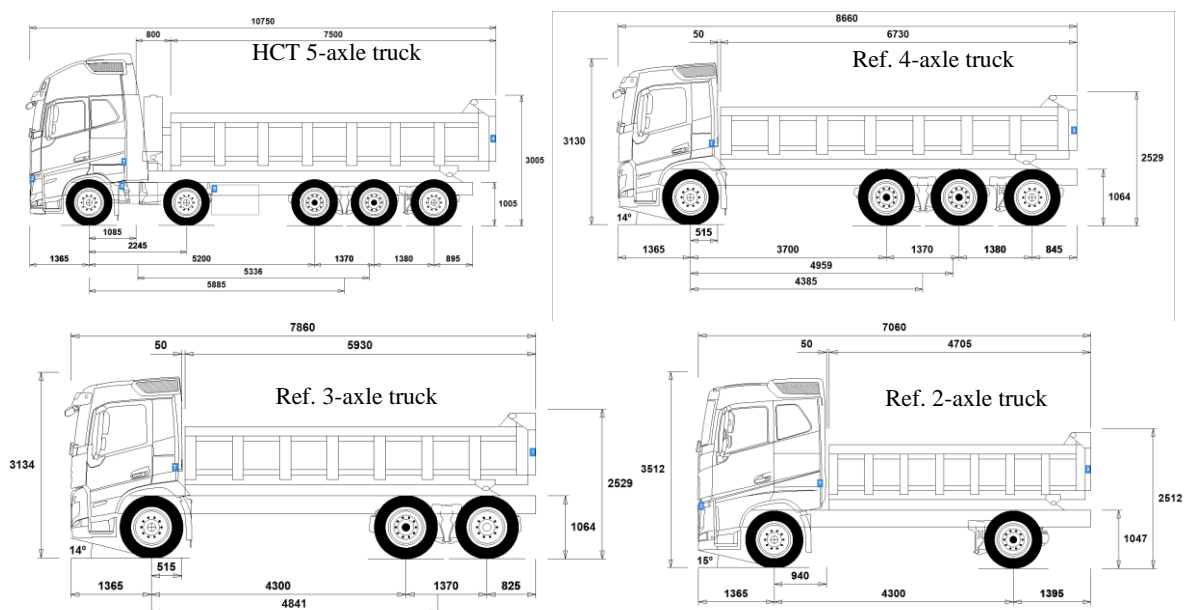


**Figure 1 – Schematic picture of the HCT truck and the three reference trucks**

**Table 1 – Relevant parameters of the trucks**

Description	HCT 5 axle truck (BK4)					4 axle truck (BK4)				3 axle truck (BK2)			2 axle truck (BK2)	
	Axle 1	Axle 2	Axle 3	Axle 4	Axle 5	Axle 1	Axle 2	Axle 3	Axle 4	Axle 1	Axle 2	Axle 3	Axle 1	Axle 2
Tire type	Single	Single	Dual	Dual	Single	Single	Dual	Dual	Single	Single	Dual	Single	Single	Dual
Tire pressure (Bar)	9	9	8	8	9	9	8	8	9	9	8	9	9	8
Axle type	Steered	Steered	Driven	Driven	Steered	Steered	Driven	Driven	Steered	Steered	Driven	Steered	Steered	Driven
		Liftable			Liftable				Liftable			Liftable		
Tire size	385/65	385/65	315/80	315/80	385/65	385/65	315/80	315/80	385/65	385/65	315/80	385/65	385/65	315/80
Axle load (loaded vehicle)	9 t	9 t	8.4 t	8.4 t	7.2 t	9 t	8.4 t	8.4 t	7.2 t	9 t	8.7 t	5.8 t	8 t	10 t
Axle load (empty vehicle) (lifted axles)	8 t	Lifted	5 t	5 t	Lifted	5.5 t	4.75 t	4.75 t	Lifted	4.7 t	7.3 t	Lifted	5 t	6 t
Axle load (empty vehicle) (no lifted axles)	4.5 t	4.5 t	3.15 t	3.15 t	2.7 t	6 t	3.1 t	3.1 t	2.8 t	5.6 t	3.9 t	2.6 t	5 t	6 t
Gross weight	42 t					33 t				23.5 t			18 t	
Empty weight	18 t					15 t				12 t			11 t	
Carried load	24 t					18 t				11.5 t			7 t	

## 2.2 The pavement structures

The relative impacts of different vehicles on a pavement structure are dependent on the mechanical properties of the structure itself. For this reason, three typical structures were analyzed to cover the possible range of road structures in Stockholm area that may be encountered by the vehicles of this study. Since the mechanical properties of pavements vary with season (due to variation in temperature and moisture), five seasons, based on pavement temperature measurements, were considered. During the spring-thaw time, the air temperature is relatively low. So, the upper AC layers of pavements are relatively stiff. But the melted ice in the bottom layers increases the moisture contents of the subgrade and the unbound base and subbase layers. This results in lowered stiffnesses of these layers. On the other hand, during the summer, the air temperature is relatively high resulting in lowered stiffnesses of the AC layers. However, the moisture content during the summer is generally much lower in the subgrade and the base and subbase layers making them relatively stiff. Thus, these two seasons represent two opposite scenarios and hence were considered important for this study.

The thicknesses and the types of materials of each layer of the three structures are presented in Figure 2. The mechanical properties of the layers, required for the analyses, were estimated based on existing laboratory test results and recommended values by the Swedish Road Administration (Trafikverket, 2011). To account for the seasonal variation of the material properties, a calendar year was divided into five seasons based on pavement temperature measurements close to Stockholm region for five years. Examples of temperature variation at 2 cm depth of a pavement during the years 2016 and 2017 are shown in Figure 3. Pavement temperature at 2 cm depth was taken as the basis for the seasonal classifications in this study. The calculations were carried out for the five seasons based on the material properties corresponding to the seasonal temperatures as presented in Table 2. Since AC is a viscoelastic material, the viscoelastic parameters of the AC layers were used for the analyses. The material properties for all these three structures were assumed to be identical. The difference was in the layer thicknesses. Structure 1 had a relatively thick (20 cm) AC layer, and a thicker unbound base layer (10 cm vs 8 cm) but a thinner unbound subbase layer (30 cm vs 42 cm) compared to Structure 2 and Structure 3. The difference between Structure 2 and Structure 3 was in the bituminous base layer thickness only. The AC layer thickness of Structure 2 was 15 cm while Structure 3 had a relatively thin AC layer of 10 cm.

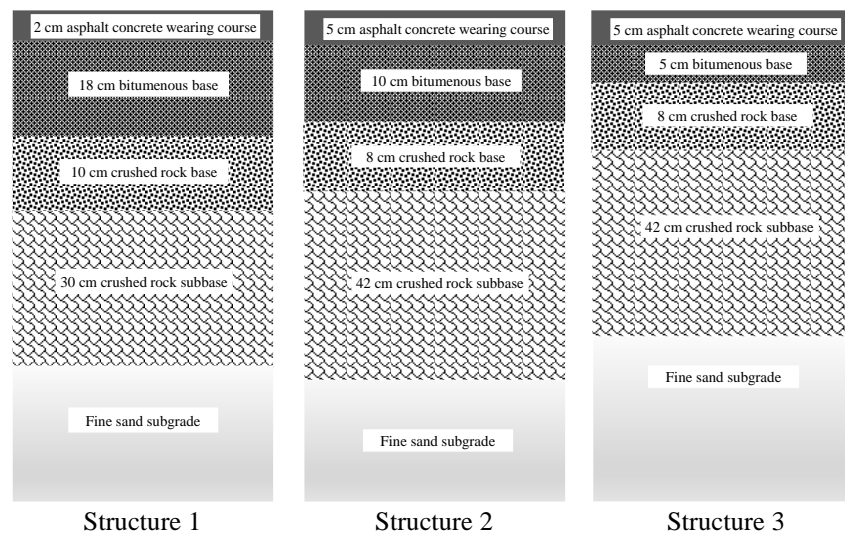


**Figure 2 – The three road structures analyzed, representative of Stockholm urban area**

**Table 2 – Assumed material properties of the different layers of the structure**

Pavement layers	Elastic modulus		Viscoelastic parameters	
	[MPa]	$D_0$	$D_1$	$m$
0°C (Winter, 3 months)				
Asphalt concrete wearing course	-	3.849E-05	0.00014945	0.3237912
Bituminous base course	-	2.9904E-05	0.00024868	0.32262286
Crushed rock base	1000	-	-	-
Crushed rock subbase	1000	-	-	-
Subgrade	1000	-	-	-
10°C (Spring-thaw, 3 months)				
Asphalt concrete wearing course	-	8.8912E-21	0.00052983	0.27327413
Bituminous base course	-	1.3142E-18	0.00068898	0.29892082
Crushed rock base	200	-	-	-
Crushed rock subbase	100	-	-	-
Subgrade	35	-	-	-
20°C (Spring and fall, 3 months)				
Asphalt concrete wearing course	-	1.8676E-11	0.00145463	0.19190149
Bituminous base course	-	5.9353E-25	0.00171103	0.2501824
Crushed rock base	300	-	-	-
Crushed rock subbase	150	-	-	-
Subgrade	100	-	-	-
30°C (Summer, 2 months)				
Asphalt concrete wearing course	-	1.8961E-11	0.00287707	0.11520106
Bituminous base course	-	1.0268E-19	0.00360265	0.19062659
Crushed rock base	300	-	-	-
Crushed rock subbase	150	-	-	-
Subgrade	100	-	-	-
40°C (Summer, 1 month)				
Asphalt concrete wearing course	-	1.1331E-19	0.00424572	0.06433834
Bituminous base course	-	3.8782E-21	0.00621811	0.13727765
Crushed rock base	300	-	-	-
Crushed rock subbase	150	-	-	-
Subgrade	100	-	-	-

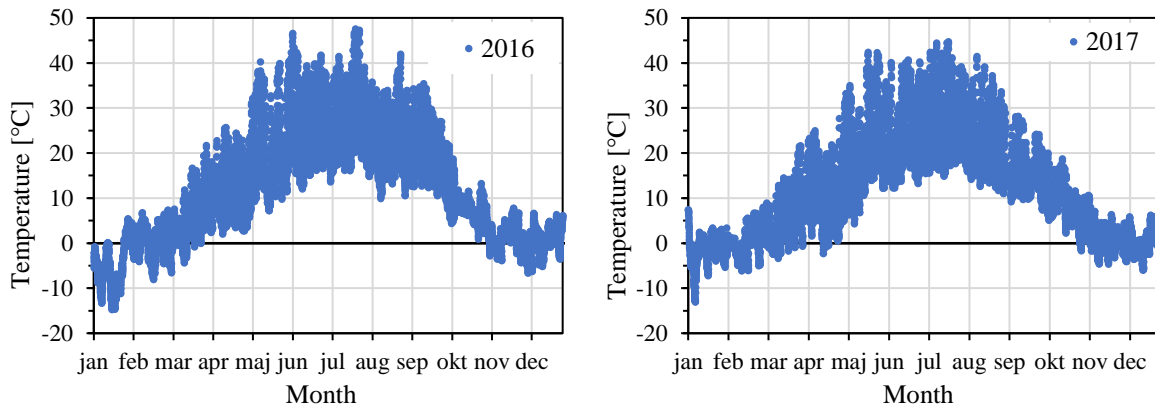


**Figure 3 – Temperature variation at 2 cm depth of a pavement close to Stockholm**

### 2.3 Analysis using ERAPave

The study was carried out in ERAPave by simulating the responses of the three pavement structures due to the passages of the four trucks. ERAPave is an axi-symmetric layered visco-elastic theory-based pavement response analysis tool. Axi-symmetric implies that the contact area between the tire and the pavement surface is assumed to be circular. Using ERAPave, the stresses and strains induced in different layers of a pavement due to moving traffic load can be calculated.

In ERAPave, the three pavement structures were modelled based on their layer thicknesses and material properties (for the five seasons considered). The vehicles were modelled using their respective axle loads and configurations, tire pressure and speed. The distances between the wheels and wheel types (single or dual tires) were used as inputs using a coordinate system. For the calculations, half axle loads (that is, wheel loads) were used. A reference speed of 45 km/hour was considered which mostly affects the viscoelastic behavior of the AC layers. Using the pavement and vehicle models in ERAPave, the stress and strain induced in the different layers of the structures were calculated.

### 3. Results and discussions

For pavement analysis and design, two of the most common types of damages taken into consideration are the fatigue cracking of the AC layer and the permanent deformation of the subgrade (subgrade rutting). The fatigue cracking of the AC layer, also known as bottom-up cracking, occurs in proportion to the induced tensile strains at the bottom of the AC layers, mostly in the transverse direction. On the other hand, the subgrade rutting is dependent on the magnitude of the vertical strain on the top of the subgrade layer. In this study, these two failure modes of pavements were analyzed.

Using ERAPave, the transverse strains induced at the bottom of the AC layers and the vertical strains at the top of the subgrade of the three structures due to the passages of the four vehicles were calculated. Examples of the calculated strain responses in Structure 1 and 3 during the spring-thaw for the four vehicles are shown in Figures 4 and 5. In these plots, the amplitude peaks at a certain point of the structures caused by the passing of the different axles of the vehicles can be seen. The viscoelastic responses of the AC layers are manifested by the delayed dwindling of the peaks as the wheels pass over that point.

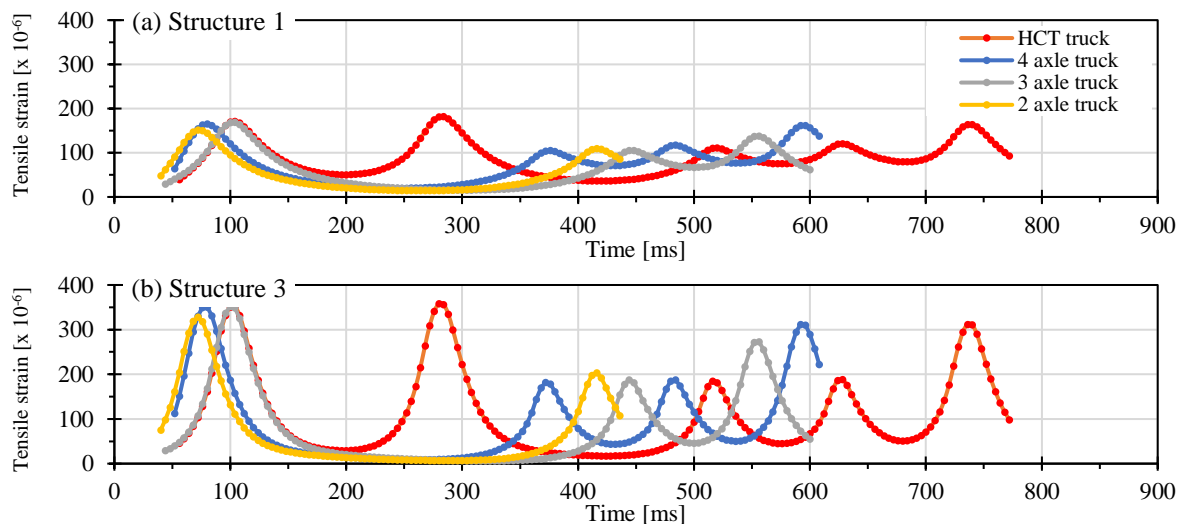


**Figure 4 – Transverse tensile strains at the bottom of the AC layer due to single passage of the fully loaded vehicles during the spring-thaw period (10°C)**

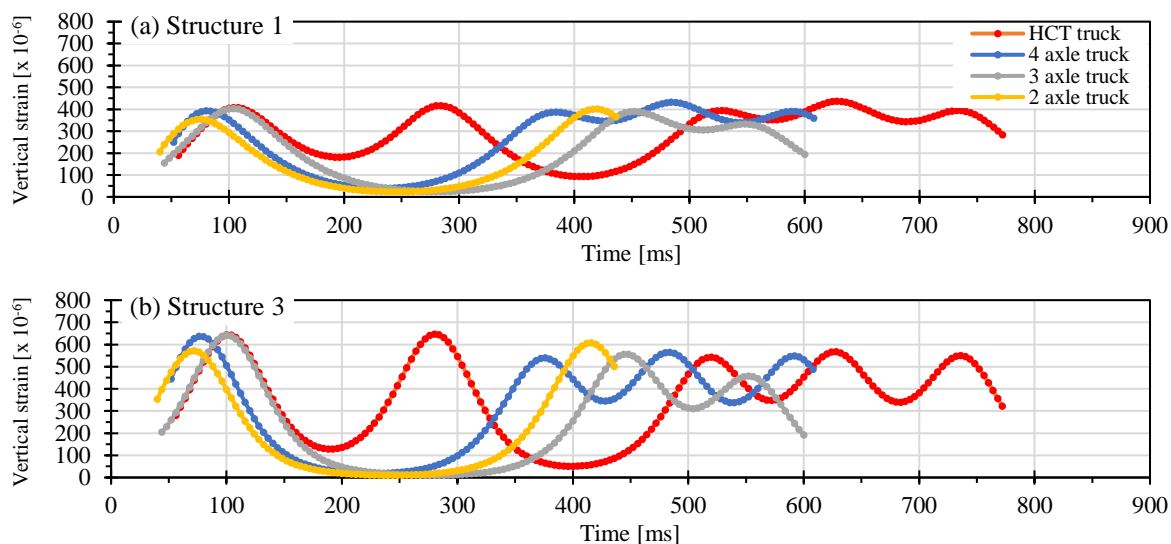


**Figure 5 – Vertical strains at the top of the subgrade due to single passage of the fully loaded vehicles during the spring-thaw period (10°C)**

The relative damage of the AC layer and the subgrade caused by the different vehicles can be calculated based on the Asphalt Institute Method (Huang, 2004). According to the AC fatigue criterion, the allowable number of load repetitions to control bottom-up cracking can be expressed as

$$N_t = a_t(\varepsilon_t)^b \tag{1}$$

According to the permanent deformation criterion, the allowable number of load repetitions to control permanent deformation of the subgrade can be expressed as

$$N_v = a_v(\varepsilon_v)^b \tag{2}$$

where,  $N_t$  and  $N_v$  are the allowable number of load cycles for AC fatigue cracking and subgrade rutting, respectively.  $\varepsilon_t$  is the transversal tensile strain at the bottom of the AC layer,  $\varepsilon_v$  is the vertical compressive strain at the top of the subgrade and  $a_t$ ,  $a_v$  and  $b$  ( $b$  is usually taken as 4) are material constants.

The damage ratio ( $D$ ) for a particular failure mode of a pavement structure is defined as a sum of the ratios between the predicted number of load repetitions  $n_i$  and the allowable number of load repetitions  $N_i$  for load  $i$  ( $i = 1, 2, \dots, m$  where  $m$  is the total number of load cases) calculated using Equation (1) or (2) as follows:

$$D = \sum_{i=1}^m \frac{n_i}{N_i} \quad (3)$$

To compare the damage caused by the single trip of a vehicle with respect to the single trip of a reference vehicle, a relative damage factor per trip ( $D_{r1}$ ) can be defined as the ratio between their respective damage ratios. In this study, the 2-axle truck was considered as the reference vehicle. Thus, for the different vehicles, the damage factors per trip becomes:

$$D_{r1} = \frac{D_j}{D_2} = \frac{(\varepsilon_1^4 + \varepsilon_2^4 + \dots + \varepsilon_j^4)_{j\text{-axle truck}}}{(\varepsilon_1^4 + \varepsilon_2^4)_{2\text{-axle truck}}} \quad (4)$$

where,  $D_2$  and  $D_j$  are the damage ratios for the 2-axle vehicle and the vehicle with  $j$  number of axles, respectively.  $\varepsilon_k$  is the magnitude of the peak strain corresponding to the  $k$ -th axle ( $k = 1, 2, \dots, j$ ) of the vehicle.

Since the load carrying capacities of the vehicles are different, they will require different numbers of trips to carry the same amount of load. Thus, for fair comparisons, the damage factors should be computed based on the number of trips required to carry the same amount of load. Since the number of trips to carry a particular amount of load would be inversely proportional to the load carrying capacity, the  $D_r$  values per unit of carried load were computed as:

$$D_r = \frac{(\varepsilon_1^4 + \varepsilon_2^4 + \dots + \varepsilon_j^4)_{j\text{-axle truck}}}{(\varepsilon_1^4 + \varepsilon_2^4)_{2\text{-axle truck}}} \left( \frac{w_2}{w_j} \right) \quad (5)$$

where,  $w_2$  and  $w_j$  are the load carried by the reference 2-axle truck and the  $j$ -axle truck, respectively.

For the round trips, two scenarios were considered. One scenario was when the vehicles returned empty without lifting any of the axles and the other scenario was when the vehicles returned empty with lifting the liftable axles (see Table 1). The  $D_r$  values for the round trips were calculated by summing up the damage caused by the loaded state and the unloaded state.

Two damage factors were defined for the two failure modes: (a) for AC fatigue cracking and (b) for subgrade rutting. For any vehicle,  $D_r < 1$  means that the vehicle is less damaging than the 2-axle vehicle and  $D_r > 1$  means that the vehicle is more damaging than the 2-axle vehicle. For the 2-axle truck,  $D_r = 1$ .



The induced strains and the  $D_r$  values for a structure can vary depending on the temperature and moisture. In Table 3, the  $D_r$  values for Structure 1 at five different pavement temperatures (the corresponding moisture contents were also different) are shown as an example to illustrate the effect of temperature on  $D_r$ . Also, to comprehend how damaging the vehicles are for Structure 1 in different seasons, the sum of the fourth powered strains (as in Equation 4) are presented. It is observed that the  $D_r$  values for AC fatigue cracking for the HCT truck are relatively higher for 0°C and 10°C, but the induced strains are relatively lower during those seasons. This indicates that these higher values of  $D_r$  are less significant. On the other hand, the  $D_r$  values as well as the induced strains in the subgrade during the spring-thaw (10°C) for the HCT truck and the 4-axle truck are higher. This is due to the weaker state of the unbound layers and the subgrade because of high water content from the thawing. The stresses from the different axles are then superposed to induce higher strains in the subgrade from the trucks with higher number of axles. Thus, during the spring-thaw period, passes of the heavier HCT truck and the 4-axle truck may need to be controlled.

To compare how damaging the vehicles are during the whole year, the yearly  $D_r$  values were calculated by summing up the damages done by the vehicles in different seasons and weighing in the durations of the seasons as:

$$D_{r,yearly} = \frac{\sum [M_k (\sum \varepsilon^4)_{j,M_k}]}{\sum [M_k (\sum \varepsilon^4)_{2,M_k}]} \left( \frac{w_2}{w_j} \right) \quad (6)$$

where,  $M_k$  is the number of months with temperature  $k$ ,  $(\sum \varepsilon^4)_{j,M_k}$  and  $(\sum \varepsilon^4)_{2,M_k}$  are the summation of fourth powered peak strains during the month with temperature  $k$  for the  $j$ -axle truck and the 2-axle truck, respectively. The  $D_{r,yearly}$  values for the three structures are presented in Figure 6. It should be noted that the plots in Figure 6 represent the relative damage risks (normalized) of the vehicles with respect to the 2-axle truck. The values do not represent which structure or season is more prone to damage.

**Table 3 – Variation in strains and  $D_r$  values for Structure 1 due to seasonal variation**

Loaded vehicles one way trip					
Temperature (°C)	0	10	20	30	40
Duration (month)	3	3	3	2	1
Summation of fourth powered peak strains ( $\times 10^{-18}$ ) per ton carried load (AC fatigue cracking)					
HCT truck	0.34	126.45	228.13	545.58	2460.83
4 axle truck	0.27	96.52	183.32	458.14	2114.32
3 axle truck	0.34	112.35	235.93	591.64	2848.07
2 axle truck	0.32	96.13	229.82	606.10	2949.83
Summation of fourth powered peak strains ( $\times 10^{-18}$ ) per ton carried load (Subgrade rutting)					
HCT truck	0.18	5979.77	810.24	1418.83	4442.90
4 axle truck	0.16	6184.62	737.93	1277.56	3979.27
3 axle truck	0.19	5423.94	849.07	1496.72	4832.54
2 axle truck	0.25	5989.47	1104.23	1956.04	6205.70
$D_r$ (AC fatigue cracking)					
HCT truck	1.07	1.32	0.99	0.90	0.83
4 axle truck	0.84	1.00	0.80	0.76	0.72
3 axle truck	1.08	1.17	1.03	0.98	0.97
2 axle truck	1.00	1.00	1.00	1.00	1.00
$D_r$ (Subgrade rutting)					
HCT truck	0.70	1.00	0.73	0.73	0.72
4 axle truck	0.63	1.03	0.67	0.65	0.64
3 axle truck	0.75	0.91	0.77	0.77	0.78
2 axle truck	1.00	1.00	1.00	1.00	1.00

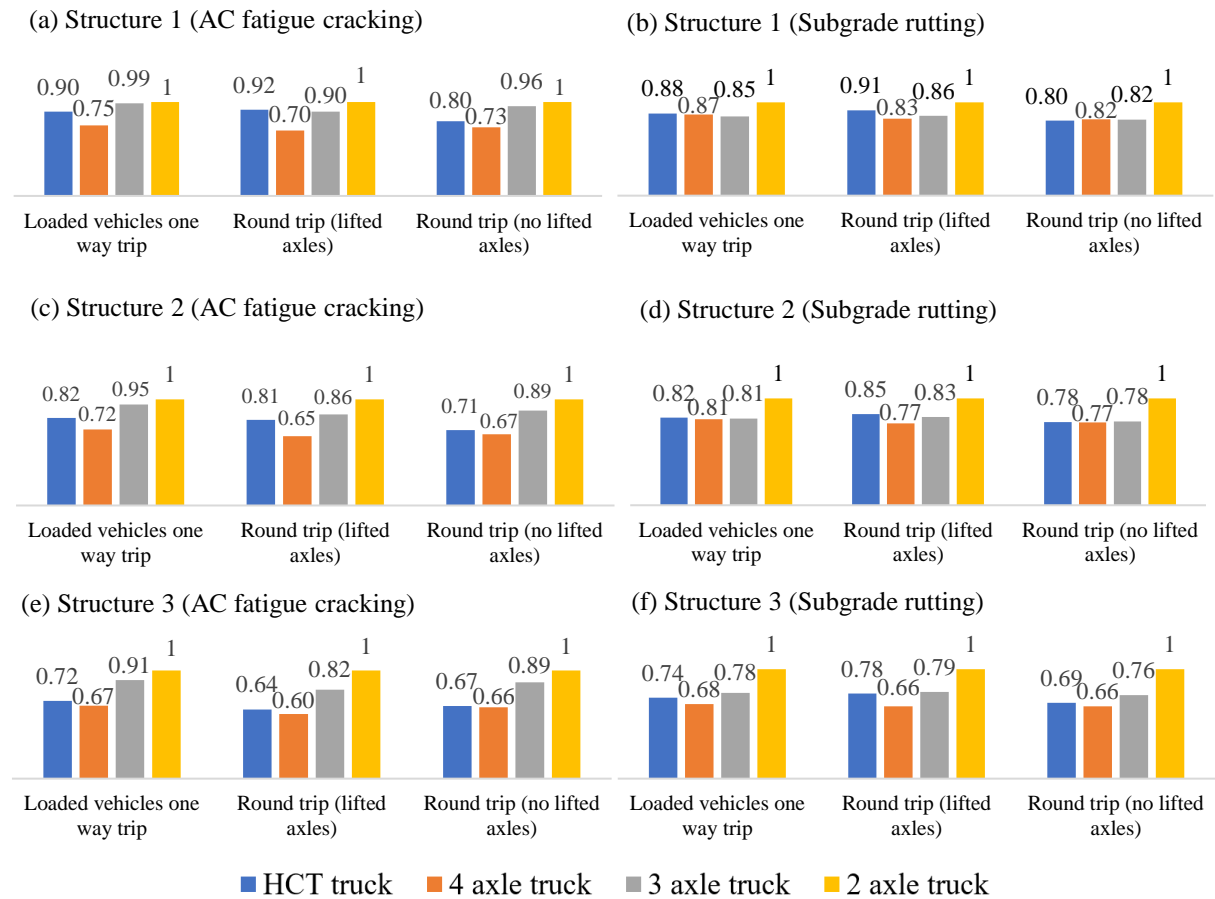


**Figure 6 –Yearly damage factor values for AC fatigue cracking and subgrade rutting**

From Figure 6, it is evident that the 4-axle truck has the lowest  $D_{r, yearly}$  values in almost all cases, meaning that it will cause the least damage to the pavements compared to the other vehicles. On the other hand, the reference 2-axle truck is the most damaging one having the highest  $D_{r, yearly}$  values in all situations, followed by the 3-axle truck. Generally, the HCT truck exhibits lower  $D_{r, yearly}$  values than the 2-axle and 3-axle trucks. It is relatively more damaging for the thicker structure (Structure 1) where its  $D_{r, yearly}$  values are closer to the 3-axle truck. However, it appears to become less damaging as the pavement gets thinner as in the case of Structure 2 and 3. Although the  $D_{r, yearly}$  values indicate that the HCT truck can be relatively more damaging for Structure 1 (the thickest one), this is less significant since the induced strains are then lower (due to higher AC layer thicknesses). This can be visualized from Figure 4 and Figure 5 by comparing the strains in Structure 1 and Structure 3.

The HCT truck and the 4-axle truck are similar in configuration. The HCT truck has an additional single axle mounted with single wheels to carry the additional load. By this, the load carrying capacity of the vehicle is increased by 6 tons (from 18 tons to 24 tons), whereas the axle load of the additional axle is 9 tons (see Table 1). This 9-ton axle with single wheels causes relatively high strain peaks both in the AC layer and the subgrade (see Figure 4 and 5). Since damage to the pavement is a fourth power law function of the induced strains, this has a considerable contribution to the damage factor for the HCT truck and makes the HCT truck

more damaging to the pavement compared to the 4-axle truck. It should be highlighted though that the HCT truck is less damaging compared to the 3-axle & 2-axle trucks. Moreover, the HCT truck has other advantages compared with the 2, 3 and 4-axle trucks, such as increased fuel efficiency and decreased traffic congestion which should be weighed in when assessing the overall benefit of the HCT truck.

#### **4. Conclusions**

In this study, the relative pavement damage risk of a 5-axle HCT truck was compared with three other reference trucks with fewer number of axles and less load carrying capacities. The analyses were based on simulations carried out employing the pavement analysis tool ERAPave. Three pavement structures representative of Stockholm urban area were considered since the HCT truck is used there. The analyses were conducted for various seasons by dividing the year into five seasons based on pavement temperature measurements. The yearly damage factors were calculated by weighing in the duration of the different seasons.

The results indicate that the HCT truck is slightly more damaging than the 4-axle truck but less damaging than the 3-axle and 2-axle trucks. The relative damage is dependent on the pavement structure and season. It should be highlighted though that the damage calculations include some simplifications and assumptions. For instance, the effect of tire width on the contact area is not included, which is disadvantageous for wide single tires. In other words, including tire width effects will decrease the relative difference between the HCT truck and the 4-axle truck, the magnitude of which should be further investigated in the future work. Moreover, to assess the potential benefit of the HCT truck, fuel efficiency and other factors should also be weighed in, not only the pavement damage risks. For instance, if the HCT-trucks are used instead of 3-axle trucks for carrying a fixed amount of load, the number of required trips will be reduced to half, and the reduction in fuel consumption is estimated to be about 40% (Segeberg et al. 2019).

This was a theoretical study that represents a general overview of the relative damage potentials of the different trucks. The numbers presented here are only valid for the specific cases presented here. For other situations, these numbers will vary although the ranking of the vehicles are expected to be similar. Nonetheless, further studies should focus on other specific cases with relevant real pavement structures, climatic conditions, and traffic scenarios. It should be noted that there were some simplifications made during the analyses. For instance, the tire-pavement contact area was assumed to be circular although it is almost rectangular in reality. Additionally, only one speed of the vehicles was considered. For other speeds, the results may slightly vary due to the viscoelastic nature of the AC layers. Furthermore, the damage factors were calculated based on the fourth power law function, using the maximum peak strain values, following the Asphalt Institute method. Further studies are needed to refine this approach to get a more accurate estimation of the relative damage potentials. Laboratory testing and full-scale testing with instrumented real pavement sections are necessary for this purpose.

#### **5. Acknowledgements**

The authors would like to thank Sweden's innovation agency, Vinnova, for financing this project (grant number 2020-05149). The authors also thank Emil Pettersson and Lena Larsson at Volvo Trucks for providing the vehicle information.

## 6. References

- Ahmed, A.W. and Erlingsson, S. (2017), “Numerical validation of viscoelastic responses of a pavement structure in a full-scale accelerated pavement test”, *International Journal of Pavement Engineering*, 18:1, 47-59, DOI:10.1080/10298436.2015.1039003.
- Cederstav, F., Ranäng, S., Asp, T. and Wandel, S. (2022), “High capacity city transport with intelligent access-A Swedish case study of transporting excavated material”, TRA, Lisbon, Portugal.
- Erlingsson, S. and Ahmed, A. (2013), “Fast Layered Elastic Response Program for the Analysis of Flexible Pavement Structures”, *Road Materials and Pavement Design*, Vol. 14, No. 1, pp. 196–210. <https://doi.org/10.1080/14680629.2012.757558>.
- Fredriksson, P., Nolz, C. and Seragiotto, C. (2021), “A mixed method evaluation of economic and environmental considerations in construction transport planning: The case of Ostlänken”, *Journal of Sustainable Cities and Society*, Volume 69. <https://doi.org/10.1016/j.scs.2021.102840>
- Huang, Y.H., (2004), “Pavement analysis and design”, 2nd ed. Englewood Cliffs, NJ: Prentice Hall.
- Segerborg, A., Larsson, L. and Olsson, E. (2019), “HCT City - ökad energieffektivitet med minskat CO2-utsläpp i staden”, Vinnova final report for project 2019-03096
- Sezer, A. and Fredriksson, A. (2021), “Environmental impact of construction transport and the effects of building certification schemes”, *Journal of Resources, Conservation and Recycling*, Volume 172, DOI: 10.1016/j.resconrec.2021.105688.
- Swedish Transport Agency (2018), “Legal loading – weight and dimensions regulations for heavy vehicles”.
- Trafikverket, (2011), “Trafikverkets tekniska krav Vägkonstruktion”, TRVK Väg, TRV 2011:072, <https://trvdokument.trafikverket.se/Versioner.aspx?spid=8&dokumentId=TDOK%202011%3a264> (in Swedish).
- Treiber, A. and Bark, P. (2016), “Energieffektiva transporter av massgods i stora tätorts områden och storstäder”, tfk report 2016:3.
- Treiber, A. and Bark, P. (2018), “Infrastructure Solutions for Increased Efficiency and Productivity of Construction Material transport in Cities”, HVTT 15 Conference, Rotterdam, Netherland.